CONTINUUM ELECTROMECHANICS GROUP

Electrohydrodynamic Charge Relaxation and Interfacial Perpendicular-Field Instability

by

James R. Melcher and Charles V. Smith, Jr.

Oct. 28, 1968 CSR TR-68-10

Electrohydrodynamic Charge Relaxation

and

Interfacial Perpendicular-Field Instability

by

James R. Melcher and Charles V. Smith, Jr.*

Department of Electrical Engineering

Massachusetts Institute of Technology

Summary: The small amplitude motions of a plane interface between two fluids stressed by an initially perpendicular electric field are investigated. The fluids are modeled as ohmic conductors and the convection of the surface charge caused by the dynamic interplay of interfacial electric shear stresses and the viscous stresses is highlighted. The influence of viscosity on instability growth rates in the zero-shear stress limits of perfectly conducting and perfactly insulating interfaces is described and compared to cases involving electrical shear stresses. Detailed attention is given to the instability of an interface between fluids having electrical relaxation times long compared to times of interest. It is shown that, for many common liquids, even a slight amount of surface charge makes the interface unstable at a considerably lower voltage than would be expected from theories based on the dielectrophoretic limit of no interfacial free charge. Experiments, performed using high frequency ac stresses, gradually increased dc fields, and abruptly applied dc fields, support the theoretical model. Instability conditions for two liquids having short relaxation times are developed to show shear stresses are not important unless conductivities are the same order of magnitude. In the general case, the elec-

---

* present address: Advanced Research and Development Directorate, EG & G, Inc. Bedford, Massachusetts.

tric Hartmann number is identified as an index to the dominance of the electric shear stresses over the viscous shear stresses in determining the interfacial convection of free charge. In the limit of large electric Hartmann number, the interface behaves essentially as a perfect conductor with the electric stress giving static instability.

I. INTRODUCTION

Electrohydrodynamic instability of the interface between two fluids stressed by an initially perpendicular electric field has received considerable attention.[1,2,3] Even so, there remain major disparities between experimental observations and theoretical explanations thus far developed. Such discrepancies can often be traced to the finite free charge relaxation time, which in turn leads to interfacial electric shear forces.

In order that a fluid interface stressed by an electric field be free of shear stresses, there must either be no free charge on the interface (in which case interfacial forces are entirely due to induced polarization), or the interface must be perfectly conducting. If the dynamics are influenced by the finite free charge relaxation time, neither of these limiting cases pertains; electrical shear force effects are involved. It follows that a self-consistent model for this class of interactions must include a mechanism, such as viscous shears, for placing the interface in shear-stress equilibrium.

A. Problem

To appreciate the objectives of this work, consider an experiment in which the initially flat interface between two fluids is stressed by a perpendicular electric field, as shown in Fig. 1. The uniform fields E_a and E_b in the regions (a) and (b) respectively above and below the interface are applied by means of plane electrodes parallel to the x - y plane, which are driven by a potential source. The gravitational acceleration, g, acts in the -z direction.

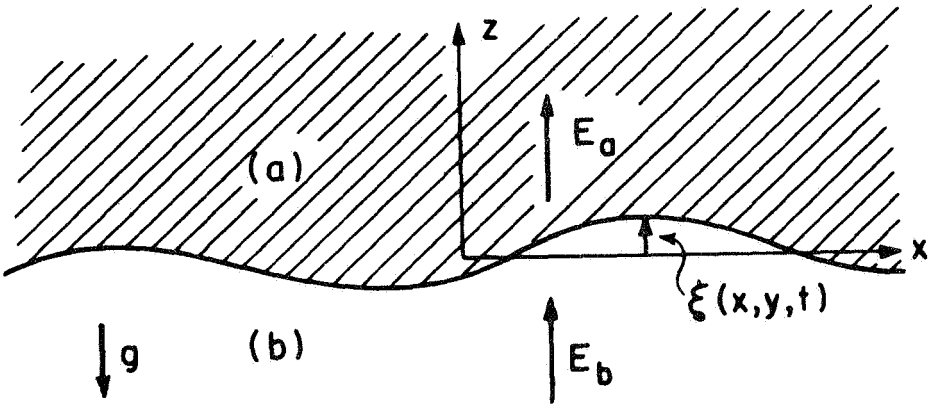

Fig. 1 Configuration of interface and applied electric field intensity.

Suppose first that the lower fluid is much more highly conducting than the upper one (water and air, for an example) and has an electrical relaxation time which is short compared to any electromechanical times of interest. It is well verified [1,2,3] that the interface is unstable at the Taylor wavelength $2\pi/k^*$ if

$$\varepsilon_a E_a^2 + \varepsilon_b E_b^2 > 2Tk^* \quad ; \quad k^* = [(\rho_b - \rho_a)g/T]^{1/2} \tag{1}$$

where ε_a and ε_b, ρ_a and ρ_b are the respective permittivities and densities and T is the surface tension. Even though this expression is based on the assumption that charge relaxation in the lower fluid is instantaneous, experiments will be described wherein Eq. (1) accurately predicts the onset of instability with fluids that are highly insulating. For example, if in an experiment using an electronegative gas and transformer oil (relaxation time about 10 sec.) the electric fields are raised slowly (over a period of minutes), the incipience of perturbations on the interface (characteristically, droplet-ejecting cusps of revolution) is predicted by Eq. (1).

The success of the perfectly conducting model in dealing with a highly insulating liquid is perhaps not surprising. According to the model, the principle of exchange of stabilities applies. With an electric stress slightly greater than that required for onset, the growth rate is very nearly zero. Although the charges relax slowly, it can be argued that they have no trouble keeping up with the interfacial dynamics, because the latter might proceed at an even slower rate. But it is more difficult to explain the observation that the time constant for instability is far shorter than the electrical relaxation time.

The perfectly conducting interface is one of two cases where there are no electric shear stresses. The second is exemplified by applying an alternating potential to the electrodes. With the period short compared to both the elec-

trical relaxation time and electromechanical times of interest, the interface does not accrue appreciable free charge and is influenced by the average of the applied electric fields. In this "dielectrophoretic limit", it is well verified [4,5] that, as the fields are raised, instability sets in as

$$(\varepsilon_a - \varepsilon_b)^2 E_a E_b / (\varepsilon_a + \varepsilon_b) = 2Tk^* \qquad (2)$$

where E_a and E_b are the rms values of the applied fields.

With the exception of highly polar liquids, the polarization instability predicted by Eq. (2) is a weak effect compared to the free charge instability of Eq. (1), in the sense that a much greater voltage is required in the second case.

Consider a third experiment which seemingly should be described by Eq. (2). Fluids are used which have long electrical relaxation times compared to the dynamical times of interest (for instance, a 10 sec. relaxation time compared to a fraction of a second for an instability to develop). The voltage is applied to the electrodes as a step after the electrodes have been shorted for many relaxation times. If the applied voltage is sufficient that Eq. (1) is satisfied, instabilities appear in a fraction of a second. This is true even though the conditions for polarization instability as given by Eq. (2) are far from satisfied. It would seem that only purely polarization effects should come into play for experiments having a duration short compared to the electrical relaxation time; however, the simple experiment does not support this view, and characterizes the type of observations that still require physical explanation.

In the following sections, the interfacial dynamics will be modeled by assuming a constant surface tension and an ohmic electrical conduction confined to the bulk of the respective fluids. On either side of the interface, the

fluids are homogeneous, with electrical conductivies σ_a and σ_b, densities ρ_a and ρ_b, and viscosities μ_a and μ_b. Hence the electrical force density in the bulk is zero, and the coupling between fluid and field is confined to the interface.[6]

B. Related Work

The ohmic, homogeneous fluid model developed here for an interface stressed by a perpendicular electric field has been used for a similar investigation of interfacial dynamics with a tangential field.[7] In that work, it is emphasized that the model can be used to understand such interfacial responses as over-stability, but only if the intrinsic bipolar conduction dominates that due to ion streaming from the electrodes. Similar limitations on the physical significance of the theory apply here, although in working with two fluids (one of which is highly insulating and in electrical "series connection" with the other) the conduction is sufficiently small to obviate the necessity for ion filters on the electrodes.

Some work[8] has been done concerning the effects of finite conductivity on the configuration of Fig. 1. However, the model used is not self-consistent, in that account is not taken of the balance of shear stresses at the interface, with viscosity brought in as a "second order" effect. For the study of parametric instabilities and other situations dominated by the normal stress dynamics of the interface, interfacial shears can possibly be ignored, but such an approach leaves in doubt the main issue of the present investigation: the role of the electrical shear stresses.

The same criticism applies to work related to the stability of cylindrical interfaces[9] where the balance of electrical shear stresses is ignored. Unless considerable foresight is used, the singular nature of the interfacial electrical

forces makes the limit of zero viscosity ambiguous and renders results based on an inviscid model meaningless. Certainly, the inviscid model cannot be used consistently in any case in which electrical shear forces are important, except in terms of an "equivalent" model which must be justified a posteriori, using the solution for the self-consistent problem.

An extreme case in which electrical shear forces are important is the one where the interface supports free charge, but where both conductors have extremely long relaxation times. Then, the interface dynamics are intimately involved with the interplay of the electrical shear forces, and the convection of charge at the interface. Here again, previous work has failed to recognize this important point[10,11] by not including the effects of electrical shear stresses and the convection of surface charge.

II. THEORETICAL MODEL

A. Bulk Dynamics

The basic electrohydrodynamic model for the fluids and their interface is the same as that used to study an interface stressed by a tangential equilibrium electric field.[7] The pertinent bulk equations are the same, and solutions are merely summarized here for the mechanical and electrical perturbations from equilibrium, defined in each region as the primed quantities

$$\begin{aligned} p &= -\rho g z + \Pi + p'(x,z,t) \\ \bar{E} &= E_o \bar{i}_z + \bar{e}'(x,z,t) \\ \bar{v} &= \bar{v}'(x,z,t) \end{aligned} \tag{3}$$

The static pressure and equilibrium electric field intensity Π and E_o differ in the two fluids and, like other variables, will be distinguished by (a) and (b).

Even with the electric field, the system is invariant to a rotation about the z axis, hence there is no loss of generality in confining attention to perturbations that are independent of y. The interface deflection from equilibrium takes the form

$$\xi = \mathrm{Re}\ \hat{\xi}\ \exp(st - jkx) \tag{4}$$

while the bulk solutions similarly are of the form

$$\bar{v}' = \mathrm{Re}\ \hat{\bar{v}}(z)\ \exp(st - jkx) \tag{5}$$

and, from Ref. 7, the complex amplitude functions of z are written in terms of the arbitrary constants, A, B, and C, as

$$\hat{v}_z = A \exp \beta z + B \exp qz \tag{6}$$

$$\hat{e}_x = C \exp \beta z \tag{7}$$

$$\hat{v}_x = - j D\hat{v}_z/k \tag{8}$$

$$\hat{p} = \mu(D^2 - k^2 - \frac{s}{\nu})D\hat{v}_z/k^2 \tag{9}$$

$$\hat{e}_z = jD\hat{e}_x/k \tag{10}$$

where $D \equiv d/dz$, $\beta = -k$ in region (a) and $\beta = k$ in region (b), with k a positive, real number. Also, $q = -q_a = -(k^2 + s/\nu_a)^{1/2}$ and $q = q_b = (k^2 + s/\nu_b)^{1/2}$ in the respective regions where q_a and q_b must have positive real parts and $\nu = \mu/\rho$.

B. Surface Coupling

The bulk solutions involve the six coefficients A, B, and C in each fluid determined by boundary conditions on the interface. A model consistent with the bulk equations requires that the normal and shear stresses on the interface be in equilibrium and that both the normal and shear velocities be continuous. Two additional conditions are provided by conservation of charge and continuity of the tangential electric field.

To write the stress conditions, it is necessary to recall that in equilibrium, the pressure distribution is hydrostatic, and that the normal equilibrium component of electric stress gives

$$\Pi^a - \Pi^b = [\![\frac{\epsilon E^2}{2}]\!] \tag{11}$$

where $[\![F]\!] \equiv F^a - F^b$. Infinitesimal perturbations are governed by the stress balance, again in the z direction

$$[\![p']\!] - g\xi[\![p]\!] - T\frac{\partial^2 \xi}{\partial x^2} = [\![\epsilon E e_z]\!] + [\![2\mu \frac{\partial v_z}{\partial z}]\!] \tag{12}$$

The balance of perturbation shear stresses requires that

$$-\frac{\partial \xi}{\partial x}[\![\epsilon E^2]\!] = [\![\epsilon E e_x]\!] + [\![\mu\left(\frac{\partial v_x}{\partial z} + \frac{\partial v_z}{\partial x}\right)]\!] \tag{13}$$

The last two equations have been linearized, so that they are to be evaluated at the equilibrium position of the interface. Since the velocity is a continuous perturbation quantity

$$[\![v_z]\!] = 0 \tag{14}$$

$$[\![v_x]\!] = 0 \tag{15}$$

The linearized x component of the condition $\bar{n} \times [\![\bar{E}]\!] = 0$ is

$$[\![e_x]\!] + \frac{\partial \xi}{\partial y} [\![E]\!] = 0 \tag{16}$$

Finally, conservation of free charge on the interface requires that

$$[\![\sigma e_z]\!] + [\![\varepsilon E]\!] \frac{\partial v_x}{\partial x} + \frac{\partial}{\partial t} [\![\varepsilon e_z]\!] = 0 \tag{17}$$

The last six equations represent the required boundary conditions. Unlike the tangential field case of Ref. 7, with the perpendicular field the equilibrium surface charge density $Q = [\![\varepsilon E]\!]$ makes a linear contribution to the conservation of charge boundary condition.

It is now a straightforward matter to substitute the solutions summarized by Eqs. (6 - 10) into the boundary conditions (12 - 17). The resulting expressions are linear and homogeneous in the coefficients $(A^a, A^b, B^a, B^b, C^a, C^b)$, and the determinant of the respective coefficients is given by Eq. (18), with

(NOTE: See page 10 for Eq. 18)

$f = g[\![\rho]\!] - Tk^2$.

C. Dispersion Equation

The compatibility condition that the determinant of the coefficients vanish is the dispersion equation. Considerable manipulation yields a form which, in the limit of no electric field, reduces to that discussed by Chandrasekhar[12].

$$-\left\{1 + \frac{gk}{s^2}(\alpha_b - \alpha_a) + \frac{Tk^3}{s^2(\rho_a + \rho_b)} + \frac{k^2 \phi [\![E]\!]}{s^2(\rho_a + \rho_b)} + \frac{ek}{d}\right\}\left\{\frac{se}{k} + \frac{\Theta [\![\varepsilon E]\!] d}{(\rho_a + \rho_b)}\right\}$$

$$+\left\{\frac{k\psi [\![\varepsilon E]\!]}{s^2(\rho_a + \rho_b)} + \frac{2k [\![\mu]\!]}{s(\rho_a + \rho_b)} - \frac{h}{d}\right\}\left\{-hs + \frac{2d [\![\mu]\!] k}{(\rho_a + \rho_b)} + \frac{\Theta kd}{(\rho_a + \rho_b)}(\varepsilon_a E_a + \varepsilon_b E_b)\right\} = 0 \tag{19}$$

$$
\begin{bmatrix}
\frac{s\rho_a}{k} - \frac{f}{s} + 2\mu_a k & \frac{s\rho_b}{k} + 2\mu_b k & -\frac{f}{s} + 2\mu_a q_a & 2\mu_b q_b & j\epsilon_a E_a & j\epsilon_b E_b \\
\frac{jk}{s}[\![\epsilon E^2]\!] + j\mu_a 2k & -j\mu_b 2k & \left[\frac{jk}{s}[\![\epsilon E^2]\!] - \frac{\mu_a q_a^2}{jk} + jk\mu_a\right] & \left[\frac{\mu_b q_b^2}{jk} - jk\mu_b\right] & -\epsilon_a E_a & \epsilon_b E_b \\
1 & -1 & 1 & -1 & 0 & 0 \\
k & k & q_a & q_b & 0 & 0 \\
-\frac{jk}{s}[\![E]\!] & 0 & -\frac{jk}{s}[\![E]\!] & 0 & 1 & -1 \\
k[\![\epsilon E]\!] & 0 & q_a[\![\epsilon E]\!] & 0 & -j(s\epsilon_a - \sigma_a) & -j(s\epsilon_b - j\sigma_b)
\end{bmatrix} = 0
$$

(18)

where

$$\alpha_a = \rho_a/(\rho_a + \rho_b) \; ; \quad \alpha_b = \rho_b(\rho_a + \rho_b)$$

$$e = \alpha_a(q_b - k) + \alpha_b(q_a - k)$$

$$h = \alpha_a(q_b - k) - \alpha_b(q_a - k)$$

$$d = (q_a - k)(q_b - k)$$

$$\phi = [\epsilon_b E_b(s\epsilon_a + \sigma_a) - \epsilon_a E_a(s\epsilon_b + \sigma_b)]/[s(\epsilon_a + \epsilon_b) + (\sigma_a + \sigma_b)]$$

$$\theta = [\![\epsilon E]\!]/[s(\epsilon_a + \epsilon_b) + (\sigma_a + \sigma_b)]$$

$$\psi = [E_a(s\epsilon_a + \sigma_a) + E_b(s\epsilon_b + \sigma_b)]/[s(\epsilon_a + \epsilon_b) + (\sigma_a + \sigma_b)]$$

The complexity of Eq. (19) reflects the variety of possible situations inherent to the model and emphasizes the necessity for relating the general case to less involved limiting situations.

III. ZERO SHEAR-STRESS DYNAMICS

A. Dispersion Equation

As indicated in the introduction, there are two commonly encountered limiting cases in which the interface is free of shear stresses. It is helpful to identify and develop these limiting cases so that they can be placed in contrast with the more involved situations in which shear effects are important. With the lower fluid sufficiently highly conducting, relative to the upper one, that $E_b \ll E_a$ and $\epsilon_a s/\sigma_a \ll 1$, we have $\phi \to -\epsilon_a E_a$, $\theta \to 0$, and $\psi \to 0$ so that

$$\left\{1 + \frac{1}{s^2}\left[gk(\alpha_b - \alpha_a) + \frac{T k^3}{(\rho_a + \rho_b)} - k^2 V_I^2\right] + \frac{ek}{d}\right\}\frac{s^2 ed}{k} - \left[\frac{2k[\![\mu]\!]d}{(\rho_a + \rho_b)} - hs\right]^2 = 0 \tag{20}$$

where

$$V_I^2 = \varepsilon_a E_a^2/(\rho_a + \rho_b) \quad \text{(Surface at constant potential)} \quad (21)$$

In the opposite extreme, where both fluids have relaxation times ε/σ long compared to $1/|s|$ and there is <u>absolutely no free charge on the interface</u>, so that $[\![\varepsilon E]\!] = 0$, Eq. (19) again reduces to Eq. (20), but with

$$V_I^2 = \frac{(\varepsilon_a - \varepsilon_b)^2 E_a E_b}{(\rho_a + \rho_b)(\varepsilon_a + \varepsilon_b)} \quad \text{(Insulating liquids, no free surface charge)} \quad (22)$$

These two classes of interaction are referred to as EH-If and EH-Ip in Ref. 2. The dispersion equation accounts for the effects of viscosity, but because the electrical forces are always normal to the interface, the effects of the electric stress are similar to those of gravity and surface tension. Note that there is no "equivalent surface tension", since the dependence of the electric contribution in Eq. (20) is on k^2, whereas that of the surface tension term is on k^3.

B. Exchange of Stabilities

For a disturbance with a given wavelength, the electrical contribution to Eq. (20) can be grouped with the gravity and surface tension terms. This makes it evident that the principle of exchange of stabilities applies just as it does in the absence of V_I (Ref. 12, page 447). Thus, the limit of Eq. (20) as $s \to 0$ represents the condition for incipient instability

$$k^2 - V_I^2 \left(\frac{\rho_a + \rho_b}{T}\right) k + \frac{g(\rho_b - \rho_a)}{T} = 0 \quad (23)$$

As the electric stress is raised, Eq. (23) shows that the Taylor wavelength $2\pi/k^*$ is the first to become unstable, with a threshold

$$V_I^2 = k^* \left(\frac{2T}{\rho_a + \rho_b}\right); \quad k^* = \sqrt{\frac{g(\rho_b - \rho_a)}{T}} \quad (24)$$

It should be clear from this discussion that, insofar as incipience of instability is concerned, previous work on zero shear stress interactions based on an inviscid model pertains.[1,2]

C. Growth Rates: Liquid and a Gas

The case of a liquid and a gas is particularly important. Common examples are air and water, in which Eq. (21) is appropriate, or Freon and its vapor in a high-frequency electric field, where Eq. (22) is appropriate. The kinematic viscosities are on the same order; hence $q_a \tilde{\sim} q_b$ while $\mu_a << \mu_b$. In normalized form, Eq. (20) then becomes

$$\left\{\frac{\underline{s}^2}{\underline{k}} + 1 + \underline{k}^2 - \underline{k}\,\underline{P}^2 + \frac{\underline{s}^2}{\underline{q}-\underline{k}}\right\}\underline{s}^2 - (\underline{q}-\underline{k})[(\underline{q}-\underline{k})\underline{s}\underline{M}]^2 \tag{25}$$

where $\rho_b = \rho$, $q_b = q$, $\rho_a = 0$ so that the normalization which reflects the essential role of the Taylor wavelength $2\pi/k^*$, is

$$\begin{aligned} \underline{k} &= k/k^* \ , \quad \underline{q} = q/k^* , \quad \underline{s} = s(T/\rho g^3)^{1/4} \\ \underline{M} &= \mu(g/\rho T^3)^{1/4} \ , \quad \underline{P} = V_I\,(\rho/k^* T)^{1/2} \end{aligned} \tag{26}$$

Note that this represents both of the zero shear cases by simply identifying $\underline{P}$ with the appropriate V_I [Eq. (21) or (22)].

In section V, it will be shown that Eq. (25) is a special case of the general one where the relaxation times in both fluids are extremely long compared to dynamical times of interest. There, a seventh order polynomial in $\underline{q}$ is given which is obtained by expanding Eq. (25), using the definition $\underline{s} = \underline{M}(\underline{q}^2 - \underline{k}^2)$ to eliminate $\underline{s}$. Thus, Eq. (26) is solved numerically for $\underline{q}$, which in turn gives $\underline{s}$.

The dependence of $\underline{s}$ on $\underline{k}$ with $\underline{P}$ as a parameter is illustrated with Fig. 2a, which is based on data for a relatively inviscid liquid (10 cs transformer oil), and Fig. 2b, computed with $\underline{M}$ increased by a factor of 10^2.

The two sets of curves in Fig. 2a are for $\underline{P}$ slightly less and somewhat greater than the $\sqrt{2}$ required for instability. Indicated on the axes are the wavenumbers $\underline{k} = \underline{k}_{u,\ell} = \underline{P}^2/2 \pm [(\underline{P}^2/2)^2 - 1]^{1/2}$ that bound the unstable band of wavenumbers, the wavenumber for maximum rate of growth $\underline{k} = \underline{k}_m = (\underline{P}^2/3) + [(P^2/3)^2 - 1/3]^{1/2}$ and the maximum rate of growth $\underline{s}_m$, all predicted by the inviscid theory. Note that there is little effect on any of these quantities from the finite viscosity $\underline{M}$, at least in the range shown. By contrast, if $\underline{M}$ is increased by a factor of 10^2, the dynamics are altered considerably (Fig. 2b). Waves with $\underline{P} = 2$ and $\underline{k}$ small are at first stable and represented by a complex conjugate pair of roots which, with increasing $\underline{k}$, switch to two purely damped modes. These in turn become one purely damped and one purely growing mode; finally, at high wavenumbers, they become two modes of a purely damped character.

IV. INFINITE RELAXATION TIME LIMIT: LIQUID AND A GAS

An important case in which shear forces can play an essential role arises when both fluids have relaxation times ε/σ that are very long compared to $1/|s|$, but there is an equilibrium surface charge on the interface. Then, any distortion of the interface must be accompanied by an electrical shear stress, and an attendant surface convection.

A. Dispersion Equation

In particular, consider the case of a liquid and a gas, so that in Eq. (19) not only are $\sigma_a \to 0$, $\sigma_b \to 0$, $\varepsilon_a = \varepsilon_o$, $\varepsilon_b = \kappa\varepsilon_o$, but also $\mu_a << \mu_b$, while $\nu_a \approx \nu_b$. It follows that the dispersion equation is

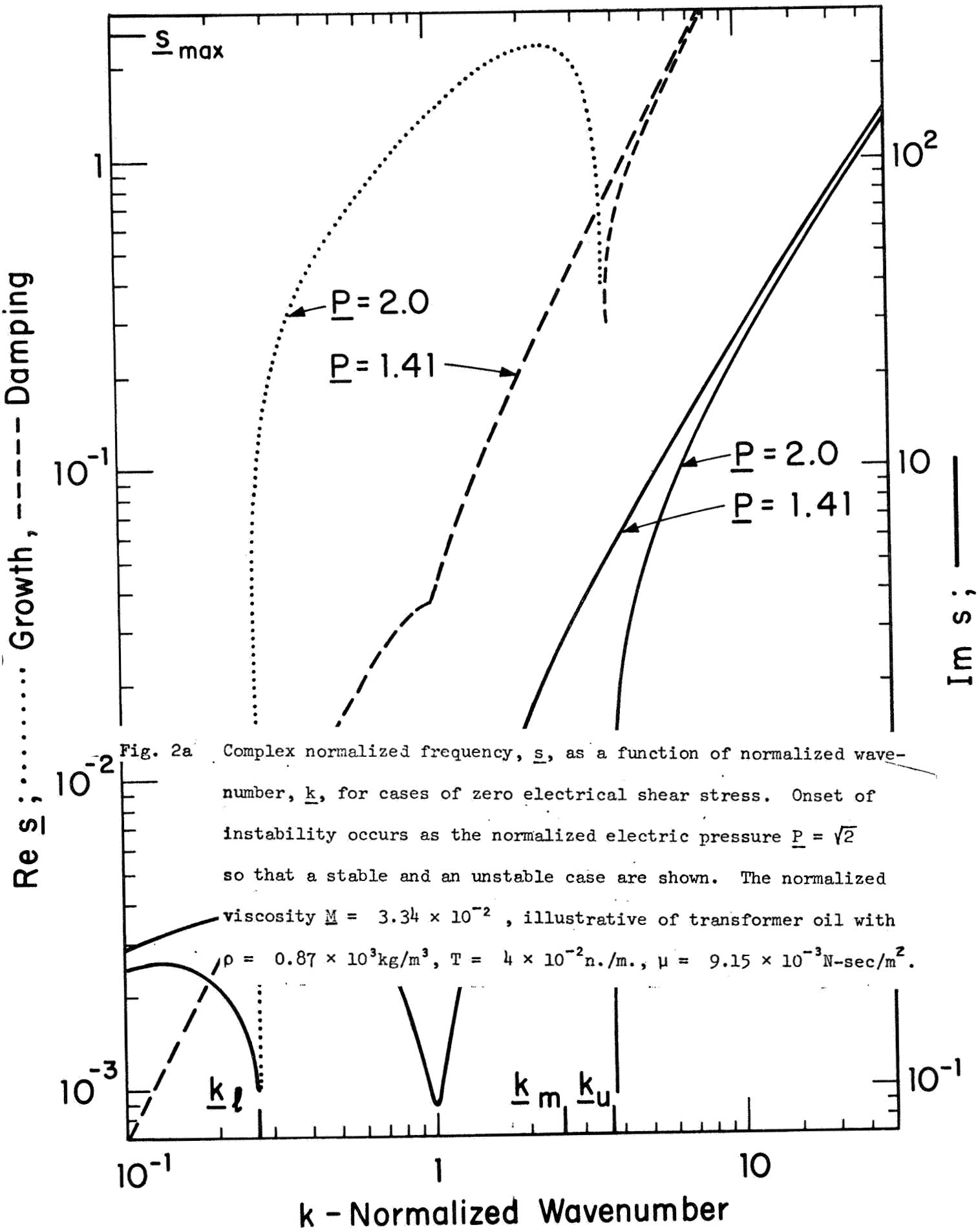

Fig. 2a Complex normalized frequency, $\underline{s}$, as a function of normalized wavenumber, $\underline{k}$, for cases of zero electrical shear stress. Onset of instability occurs as the normalized electric pressure $\underline{P} = \sqrt{2}$ so that a stable and an unstable case are shown. The normalized viscosity $\underline{M} = 3.34 \times 10^{-2}$, illustrative of transformer oil with $\rho = 0.87 \times 10^{3} kg/m^{3}$, $T = 4 \times 10^{-2} n./m.$, $\mu = 9.15 \times 10^{-3} N\text{-}sec/m^{2}$.

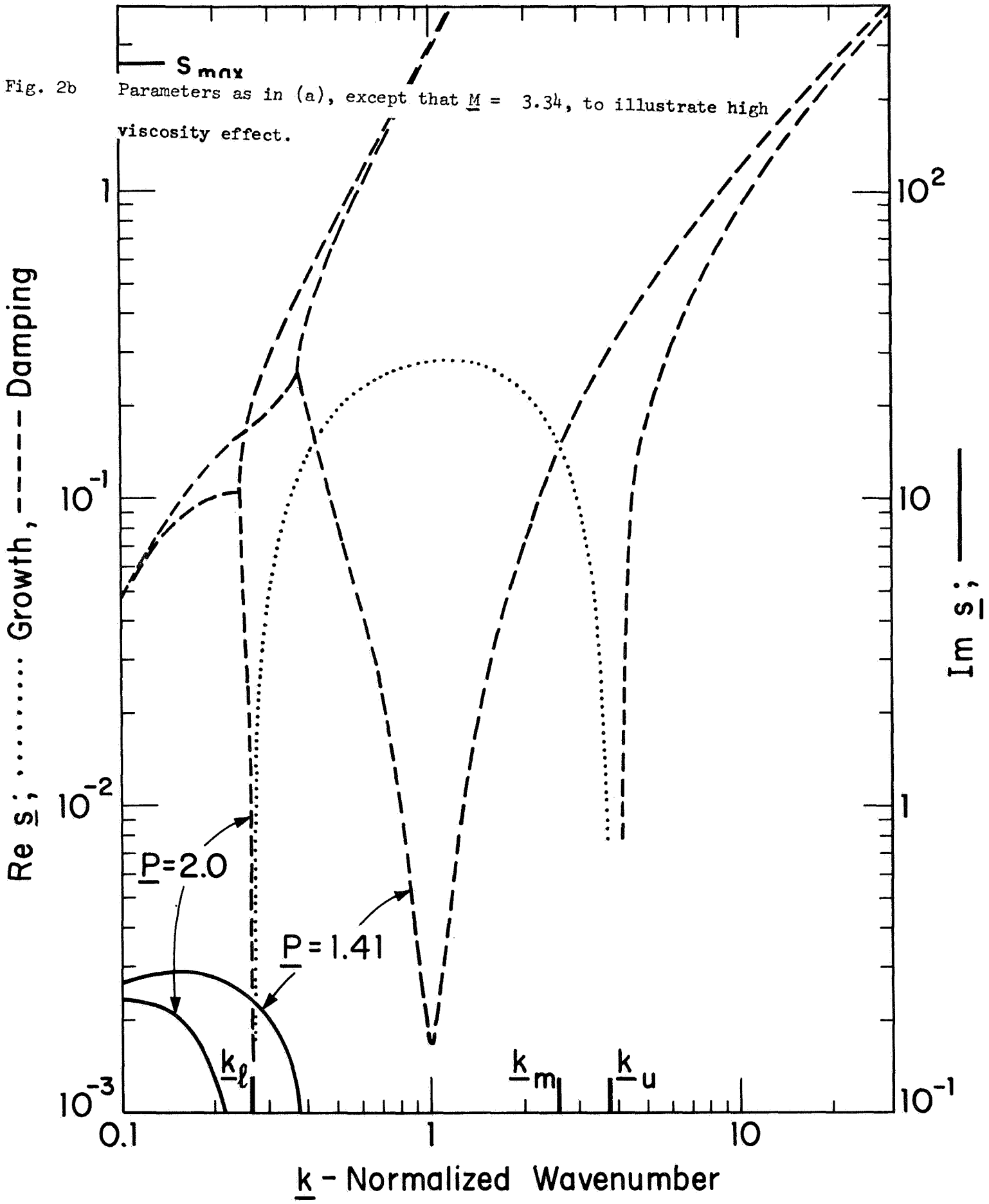

Fig. 2b Parameters as in (a), except that $\underline{M}$ = 3.34, to illustrate high viscosity effect.

$$\left\{\frac{\underline{s}^2}{\underline{k}} + 1 + \underline{k}^2 - \underline{P}^2\underline{k} + \frac{\underline{s}^2}{\underline{q}-\underline{k}}\right\}\left\{\frac{\underline{s}^2}{\underline{k}} + (\underline{q}-\underline{k})\underline{Q}^2\right\}$$

$$- \frac{(\underline{q}-\underline{k})}{\underline{k}}\left\{(\underline{k}-\underline{q})\underline{s}\,\underline{M} - \underline{k}\,\underline{W}^2\right\}^2 = 0 \qquad (27)$$

where, in addition to the normalization variables of Eqs. (26) we have

$$\begin{aligned}
\underline{P}^2 &= [\![E]\!]^2\varepsilon_o\,\kappa/k^*T(1+\kappa) \\
\underline{Q}^2 &= [\![\varepsilon E]\!]^2/Tk^*\,\varepsilon_o(1+\kappa) \qquad (28)\\
\underline{W}^2 &= \underline{Q}^2\,\frac{(1+\kappa)}{(1-\kappa)} - \frac{2\sqrt{\kappa}}{(1-\kappa)}\,\underline{P}\,\underline{Q}
\end{aligned}$$

Note that the definition of $\underline{P}$ is consistent with that in Eqs. (26), if V_I is taken as that for the case of a polarization interaction[Eq. (22)]. The variable $\underline{Q}$ is proportional to the equilibrium surface charge on the interface; as suggested in Sec. III, Eq. (27) in the limit $\underline{Q} \to 0$, and hence $\underline{W} \to 0$, reduces to Eq. (25) when this latter equation is written for the polarization case. Substitution in Eq. (27) for $\underline{s}$ in terms of $\underline{q}$ gives the dispersion equation written as a polynomial in $\underline{q}$.

$$\begin{aligned}
&\underline{q}^7[\underline{M}^4] + \underline{q}^6[\underline{k}\,\underline{M}^4] + \underline{q}^5[\underline{k}^2\underline{M}^4] + \underline{q}^4[\underline{k}\underline{M}^2\underline{Q}^2 - 3\underline{k}^3\underline{M}^4] \\
&\quad + \underline{q}^3\{\underline{M}^2[\underline{k} + \underline{k}^3 - \underline{k}^2(\underline{P}^2 - \underline{Q}^2 + 2\underline{W}^2)] - 5\,\underline{k}^4\underline{M}^4\} \\
&\quad + \underline{q}^2\{3\underline{k}^5\underline{M}^4 + \underline{k}\,\underline{M}^2[\underline{k} + \underline{k}^3 - \underline{k}^2(\underline{P}^2 + \underline{Q}^2 - 2\,\underline{W}^2)]\} \qquad (29)\\
&\quad + \underline{q}\{3\,\underline{M}^4\underline{k}^6 - \underline{k}^2\underline{M}^2[\underline{k} + \underline{k}^3 - \underline{k}^2(\underline{P}^2 - \underline{Q}^2 + 2\,\underline{W}^2)]\} \\
&\quad + \{-\underline{k}^7\underline{M}^4 - (\underline{k} + \underline{k}^3 - \underline{k}^2\underline{P}^2)(\underline{k}^3\underline{M}^2 - \underline{k}\,\underline{Q}^2) - 2\,\underline{k}^5\underline{W}^2\underline{M}^2 - \underline{k}^3\underline{W}^4\} = 0
\end{aligned}$$

Numerical solutions for $\underline{q}$'s having positive real parts in turn give $\underline{s} = \underline{M}(\underline{q}^2 - \underline{k}^2)$.

Although the physical case in which the lower fluid is perfectly conducting while the upper one is insulating is altogether different from the situation for which Eq. (29) is derived, it is represented mathematically by Eq. (29) if $\underline{Q} = \underline{W} = 0$ and $\underline{P}$ is evaluated using Eqs. (21) and (26).

B. Marginal Instability

The essential role of the electric shear stresses in the infinite relaxation time limit can be appreciated by considering the manner in which $\underline{Q}$ and $\underline{W}$ influence the exchange of stabilities. If $\underline{Q}$, and hence $\underline{W}$, are zero in Eq. (27), and then the limit is taken where $\underline{s} \to 0$, it is found that instability is first incipient at the Taylor wavelength $2\pi/k^*$ with the voltage as given by Eqs. (22) and (24). That is, the instability has the same incipient conditions as for the purely dielectrophoretic interaction with the interface, and the normalized jump in electric field intensity required for instability is

$$\underline{P} = \sqrt{2} \tag{30}$$

By contrast, if $\underline{Q}$, and hence $\underline{W}$, are finite in Eq. (27) and the limit is taken where $\underline{s} \to 0$, the Taylor Wavelength is again the first to give incipient instability, but the value of $\underline{P}$ required is only

$$\underline{P} = \sqrt{2}\left[\frac{1 - \kappa}{1 + \kappa}\right] \tag{31}$$

In general, for $\underline{Q}$ finite, exchange of stabilities is incipient with $\underline{k} = \underline{k}^*$ for $\underline{P}$ and $\underline{Q}$ satisfying

$$\underline{P}^2 - \frac{4\sqrt{\kappa}}{1 + \kappa}\underline{P}\,\underline{Q} + \underline{Q}^2 = \frac{2(1 - \kappa)^2}{(1 + \kappa)^2} \tag{32}$$

In terms of the electric field intensities at the interface, this expression is identical with

$$\varepsilon_a E_a^2 + \varepsilon_b E_b^2 = 2\,Tk^* \quad ; \tag{33}$$

a condition for incipient instability that would be obtained if the interface were regarded as perfectly conducting[2, pg. 48] and bounded on either side by perfectly insulating fluids.

The demarcation given by Eq. (32) between regimes of stability and instability in the $\underline{P}$ - $\underline{Q}$ plane is shown in Fig. 3. This figure also shows the singular regime of stability at $\underline{Q} = 0$, with a maximum $\underline{P} = \sqrt{2}$ as given by Eq. (30).

C. Dynamics

The physical significance of the contours of marginal exchange of stabilities shown in Fig. 3 is clarified by computing the complex frequencies from Eq. (29), calculations which indicate that the first instabilities to appear as the electric stress ($\underline{P}$ and $\underline{Q}$) is increased are indeed static, and satisfy the principle of exchange of stabilities.

The dependence of $\underline{s}$ on $\underline{Q}$ is characterized for low and high viscosity liquids by Figs. 4a and 4b, where $\underline{P} = 1$, a value large enough to secure instability according to condition (31), but not large enough according to Eq. (30). Hence, in terms of the $\underline{P}$ - $\underline{Q}$ plane of Fig. 3, the complex frequencies are given in Fig. 4 for a line parallel to the $\underline{Q}$ axis and passing through the points denoted (a) - (c). These points are also identified on Fig. 4. At point (a) of Fig. 4a, where $\underline{Q} = 0$, there is a single pair of complex conjugate frequencies, indicating damped oscillations. With finite $\underline{Q}$, the complex conjugate roots are retained, but in addition there is a purely real root, indicating static instability. The growth rate at first increases rapidly with $\underline{Q}$, then goes to zero as the point (b) is approached. In the range (b) - (c) the interface is again stable, but with motions represented by two complex conjugate pairs of roots. Beyond point (c) there is

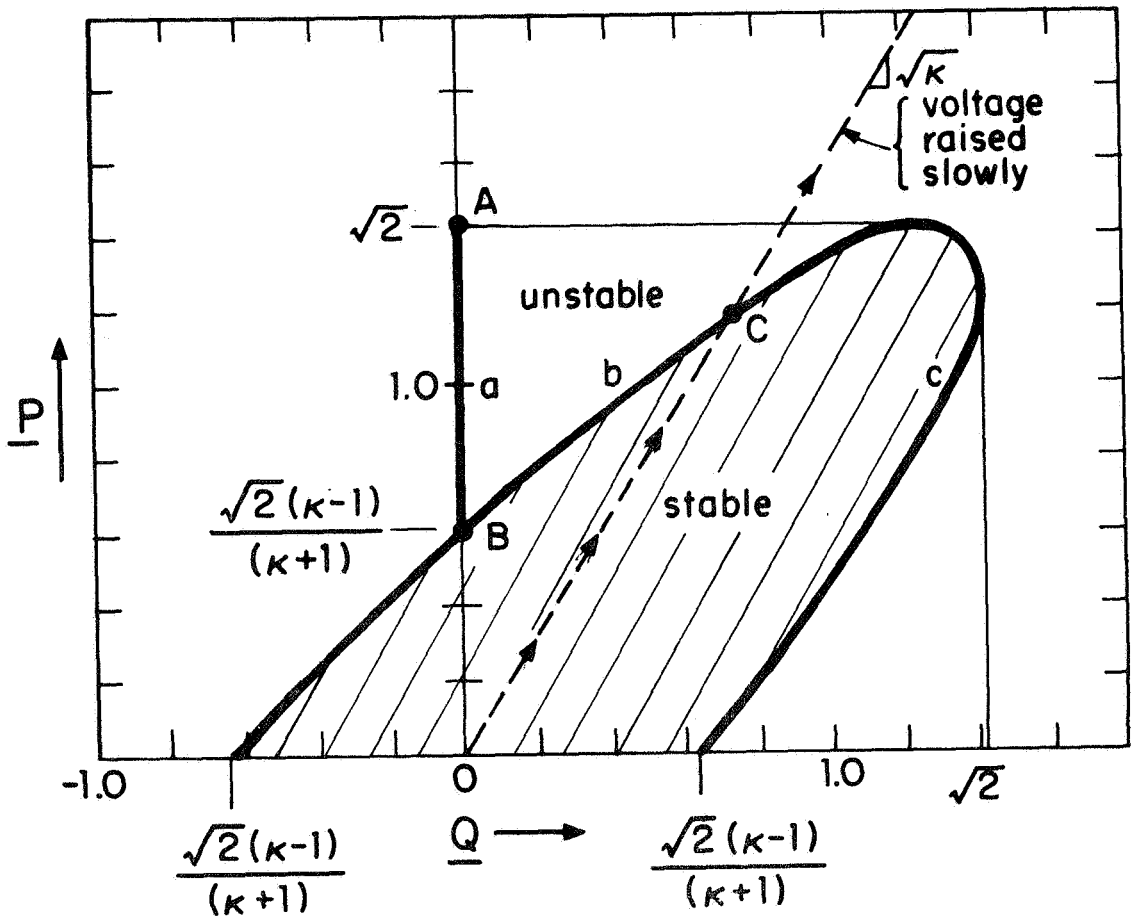

Fig. 3 Regime of stability in the P-Q plane, where Q is the normalized surface charge and P is the normalized jump in electric field intensity at the interface. As P is raised with Q = 0, polarization (dielectrophoretic) instability occurs at A, while the free charge instability occurs (asymptotically) at B. Raising the voltage slowly gives the trajectory shown, with instability at the point C. κ = 2.56, characteristic of transformer oil.

Fig. 4 Normalized complex frequencies, $\underline{s}$, as a function of surface charge density, $\underline{Q}$. Points (a) - (c) correspond to those shown on Fig. 3, where $\underline{P} = 1$.

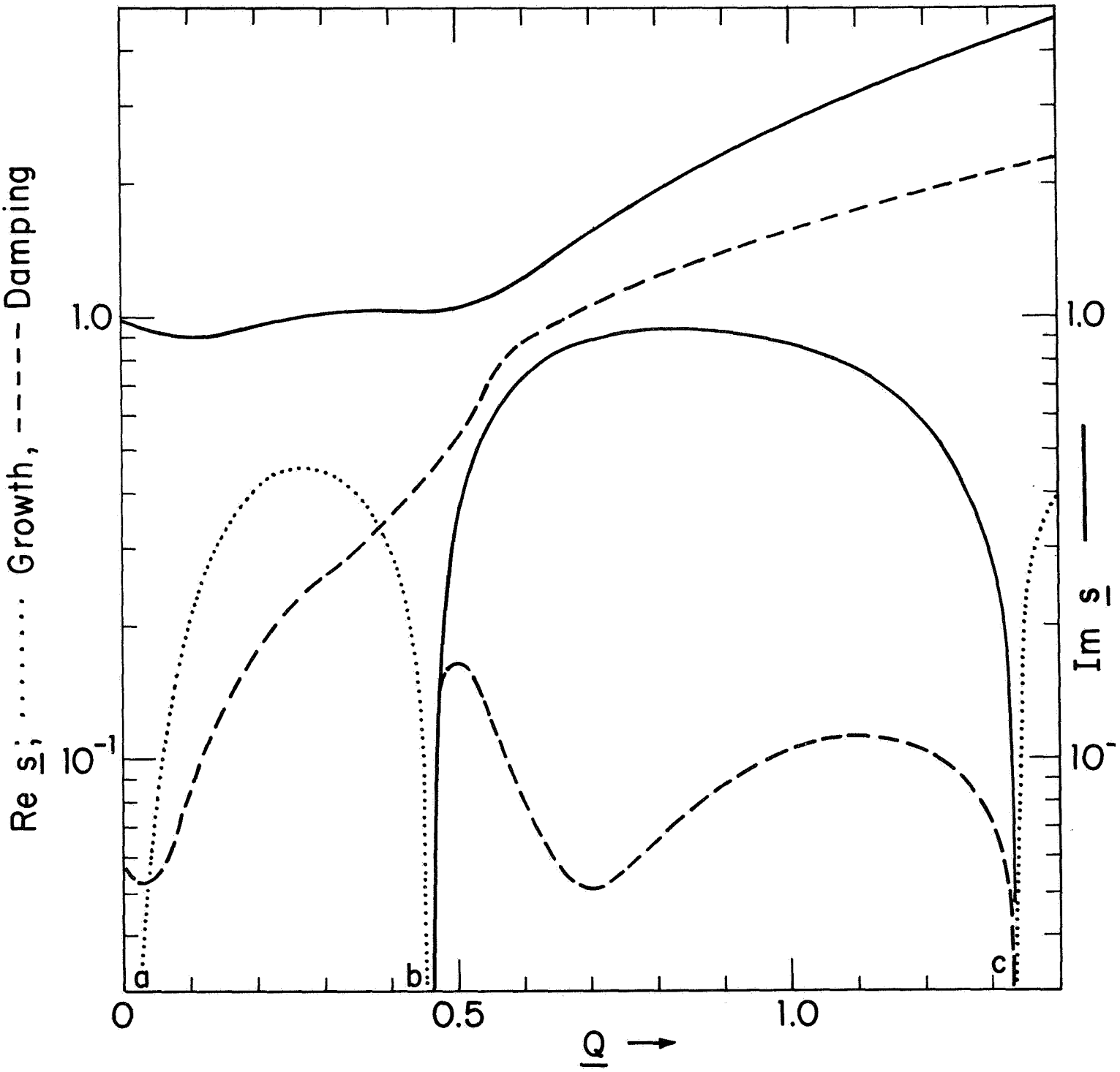

a) The viscosity is that of transformer oil, $\underline{M} = 3.34 \times 10^{-2}$. From (a)-(b) and beyond (c), there are a complex conjugate pair of roots and a purely positive real root. From (b)-(c) there are two complex conjugate pairs of roots.

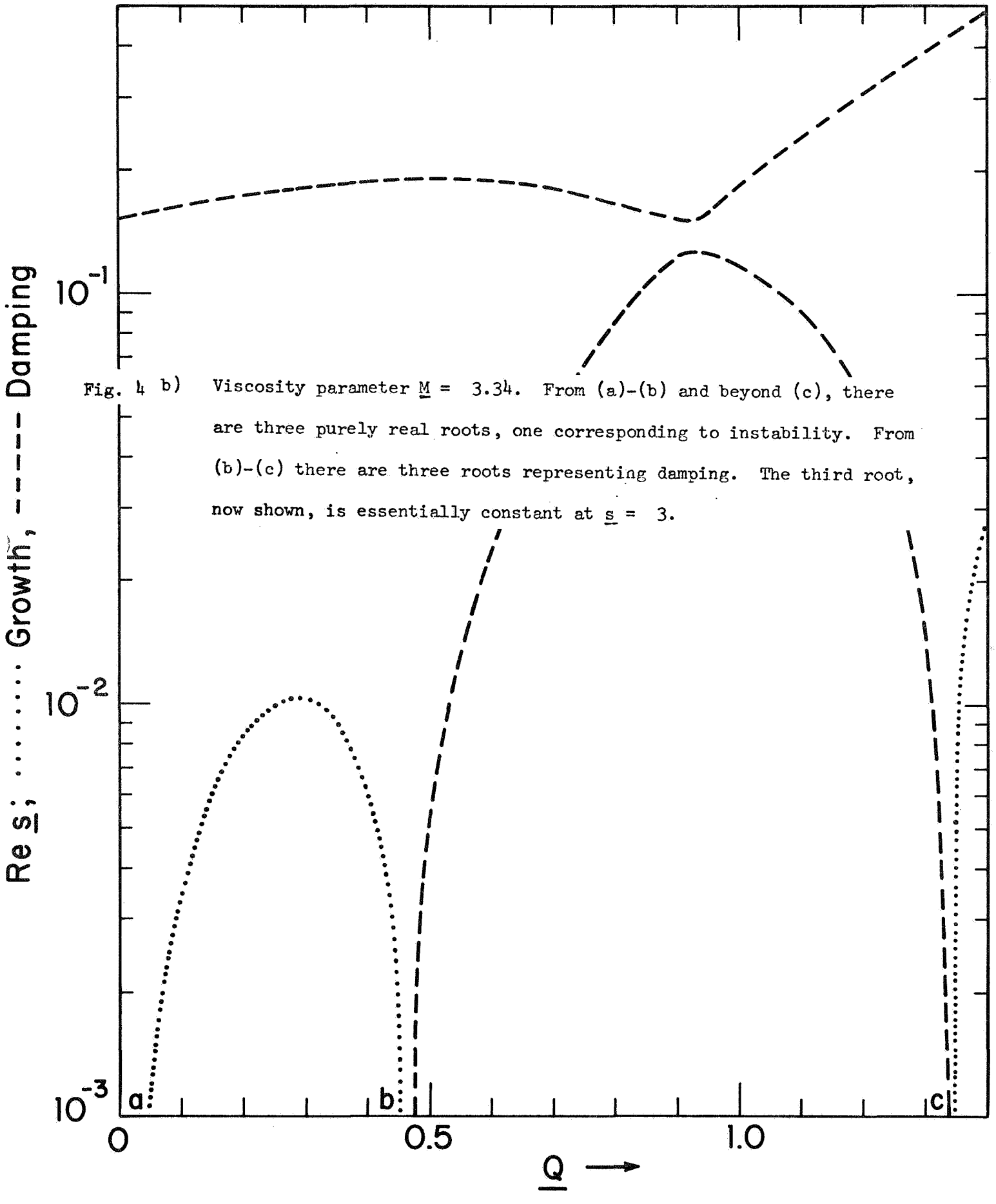

Fig. 4 b) Viscosity parameter $\underline{M}$ = 3.34. From (a)-(b) and beyond (c), there are three purely real roots, one corresponding to instability. From (b)-(c) there are three roots representing damping. The third root, now shown, is essentially constant at $\underline{s}$ = 3.

again a static instability. In the more viscous case of Fig. 4b, roots are real; one unstable and two damped from (a) - (b) and beyond (c), and three damped in the range (b) - (c).

The contours shown in Fig. 3 are those of zero growth rate or marginal instability. If Eq. (29) is solved for contours of finite constant growth rate ($\underline{s}$ = 0.2, $\underline{k}$ = 1), these appear as shown in Fig. 5. The contours tend toward the marginal stability curves as the viscosity is reduced.

The marked effect of the electrical shear stresses resulting from the combination of a finite equilibrium surface charge density, $\underline{Q}$, and a perfectly insulating liquid is now clear. Remember that the skewed ellipse of Fig. 5 is identical to the curve that would be obtained with the assumption that the interface is perfectly conducting [Eq. (32) or (33)]. With the insulating interface, charge convection replaces charge conduction in adjusting the charge distribution so that the electric field intensity remains perpendicular to the deformed interface. The remarkable fact is that the convection process can occur so rapidly in liquids like transformer oil that on the time scale of many experimental situations it is difficult to tell the difference between the perfectly conducting interface and one that is perfectly insulating. As will be pointed out in Sec. VII, this is true particularly in view of the extreme sensitivity of the stability condition to <u>small</u> amounts of equilibrium surface charge.

V. INSTANTANEOUS RELAXATION LIMIT

Consider now an extreme which is the opposite of that described in Sec. IV: the electrical relaxation times in both fluids are short compared to times $1/|s|$ of interest.

$$|s\varepsilon_a/\sigma_a| << 1, \qquad |s\varepsilon_b/\sigma_b| << 1 \tag{34}$$

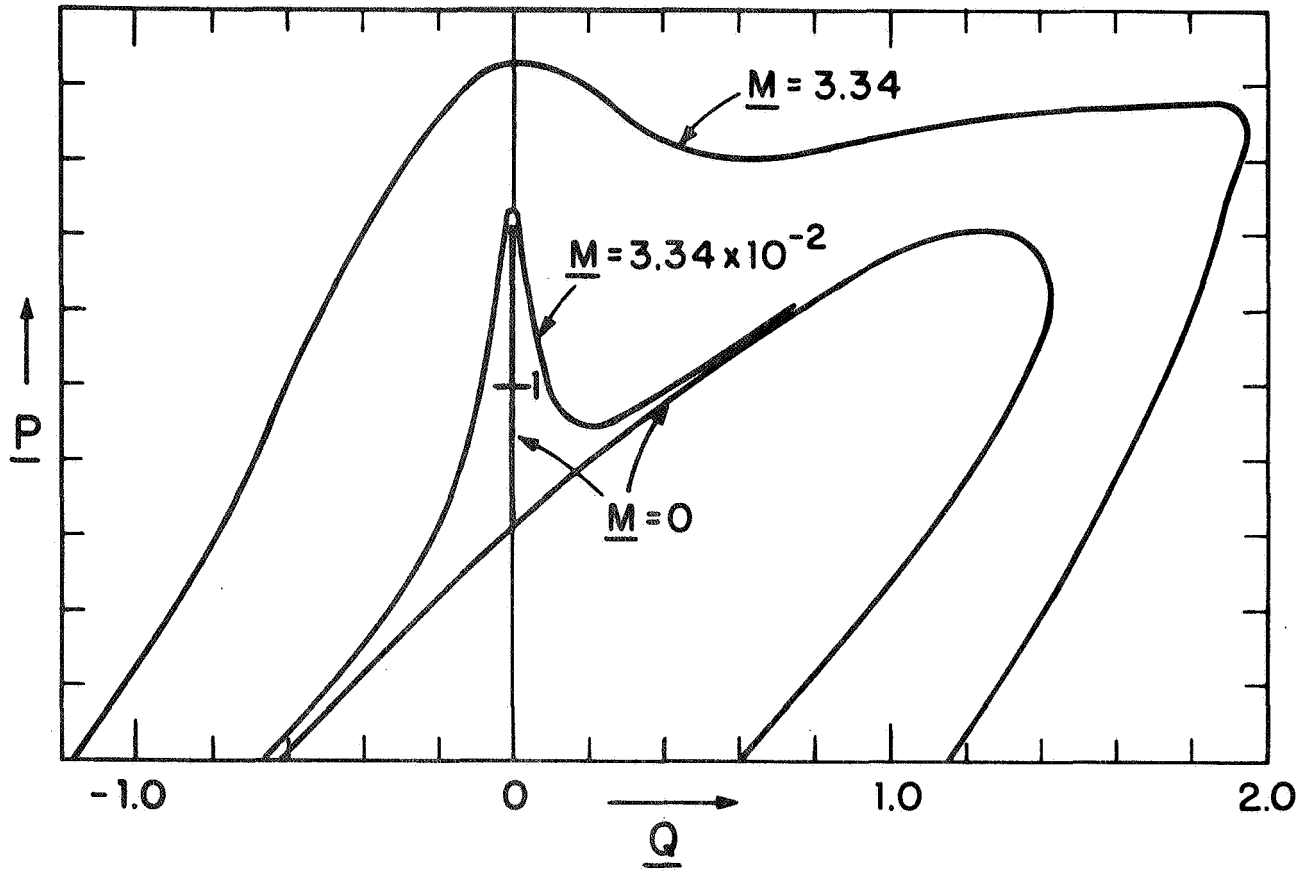

Fig. 5 Contours of constant growth rate $\underline{s}$ = 0.2, $\underline{k}$ = 1.0 in the $\underline{P}$-$\underline{Q}$ plane as a function of the viscosity parameter, $\underline{M}$. In the limit of zero viscosity, the contour becomes the marginal stability curve of Fig. 3; κ = 2.56.

In addition, it is assumed that $|s|/\nu \ll k^2$; that mechanical motions are characterized by times which are long compared to the viscous diffusion time $1/k^2\nu$. Then, Eq. (19) reduces to a simple dispersion equation which is quadratic in s.

$$(\rho_a + \rho_b)s^2 + s[2k^2(\mu_a + \mu_b)] + [gk(\rho_b - \rho_a) + Tk^3 - k^2 S] = 0 \qquad (35)$$

where

$$S = \left\{ [\![E]\!](\epsilon_a E_a \sigma_b - \epsilon_b E_b \sigma_a) + \frac{[\![\epsilon E]\!]^2(\sigma_a E_a + \sigma_b E_b)(\epsilon_a E_a + \epsilon_b E_b)}{[2(\mu_a + \mu_b)(\sigma_a + \sigma_b) + [\![\epsilon E]\!]^2]} \right\} \Big/ (\sigma_a + \sigma_b)$$

It is clear from Eq. (35) that overstability is not possible, and once again the principle of exchange of stabilities is valid. Incipience of instability occurs as the last term in Eq. (35) becomes zero.

$$k^2 - k\frac{S}{T} + (k^*)^2 = 0 \quad ; \quad k^* = \sqrt{g(\rho_b - \rho_a)/T} \qquad (36)$$

With $\rho_b > \rho_a$, the equilibrium is stable in the absence of an electric field ($S = 0$). Then, as S is raised, the first wavelength to become unstable is again the Taylor wavelength $2\pi/k^*$. The condition for instability at that most critical wavelength is

$$\frac{S}{2T} = k^* \qquad (37)$$

In this instantaneous relaxation limit, the equilibrium fields, like the perturbation fields, are determined by the conduction. Thus, $E_b = (\sigma_a/\sigma_b)E_a$, and Eq. (37) is written as

$$P_o^2 = \left\{ (1 - \alpha\Sigma) + [(1 + \alpha\Sigma)^2 + 4\delta\Sigma]^{1/2} \right\} \Big/ \gamma \qquad (38)$$

where

$$P_o^2 = \varepsilon_a E_a^2 / k^* T$$

$$\alpha = \left[\frac{\varepsilon_b}{\varepsilon_a}\left(\frac{\sigma_a}{\sigma_b}\right)^2 - 1\right]\left(1 - \frac{\sigma_b}{\sigma_a}\right) \Bigg/ \left(1 - \frac{\varepsilon_b \sigma_a}{\varepsilon_a \sigma_b}\right)^2$$

$$\delta = 2\left(1 + \frac{\varepsilon_b \sigma_a}{\varepsilon_a \sigma_b}\right) \Bigg/ \left(1 - \frac{\varepsilon_b \sigma_a}{\varepsilon_a \sigma_b}\right)^2$$

$$\gamma = 1 + \frac{\varepsilon_b}{\varepsilon_a}\left(\frac{\sigma_a}{\sigma_b}\right)^2$$

$$\Sigma = (\mu_a + \mu_b)\sigma_a / \varepsilon_a \, Tk^*$$

The dependence of P_o^2 on the ratio of conductivities σ_a/σ_b, as given by Eq. (38), is illustrated in Fig. 6. For either $\sigma_a/\sigma_b >> 1$ or $\sigma_a/\sigma_b << 1$, P_o^2 approaches a value that is predicted by using a model that assumes the interface to be perfectly conducting and hence free of electrical shear stresses [Eq. (33)]. However, in the range where the conductivities are on the same order, the electrical shear stresses come into play to a degree that depends on the viscosity parameter, Σ.

It is interesting to note that in the particular limiting case in which $\sigma_a/\sigma_b \to \varepsilon_a/\varepsilon_b$, so that there is no equilibrium interfacial charge, Eq. (38) becomes

$$P_o^2 = 2(\sigma_a/\sigma_b + 1)/(\sigma_a/\sigma_b - 1)^2 \qquad (39)$$

as can most easily be shown by resolving Eq. (37) for P_o^2 after taking the limiting case. Because Eq. (39) is valid only if $\sigma_a/\sigma_b = \varepsilon_a/\varepsilon_b$, this is the same condition as given by Eqs. (22) and (24). Thus, due to the polarization interaction discussed in Sec. III, the interface has a threshold for

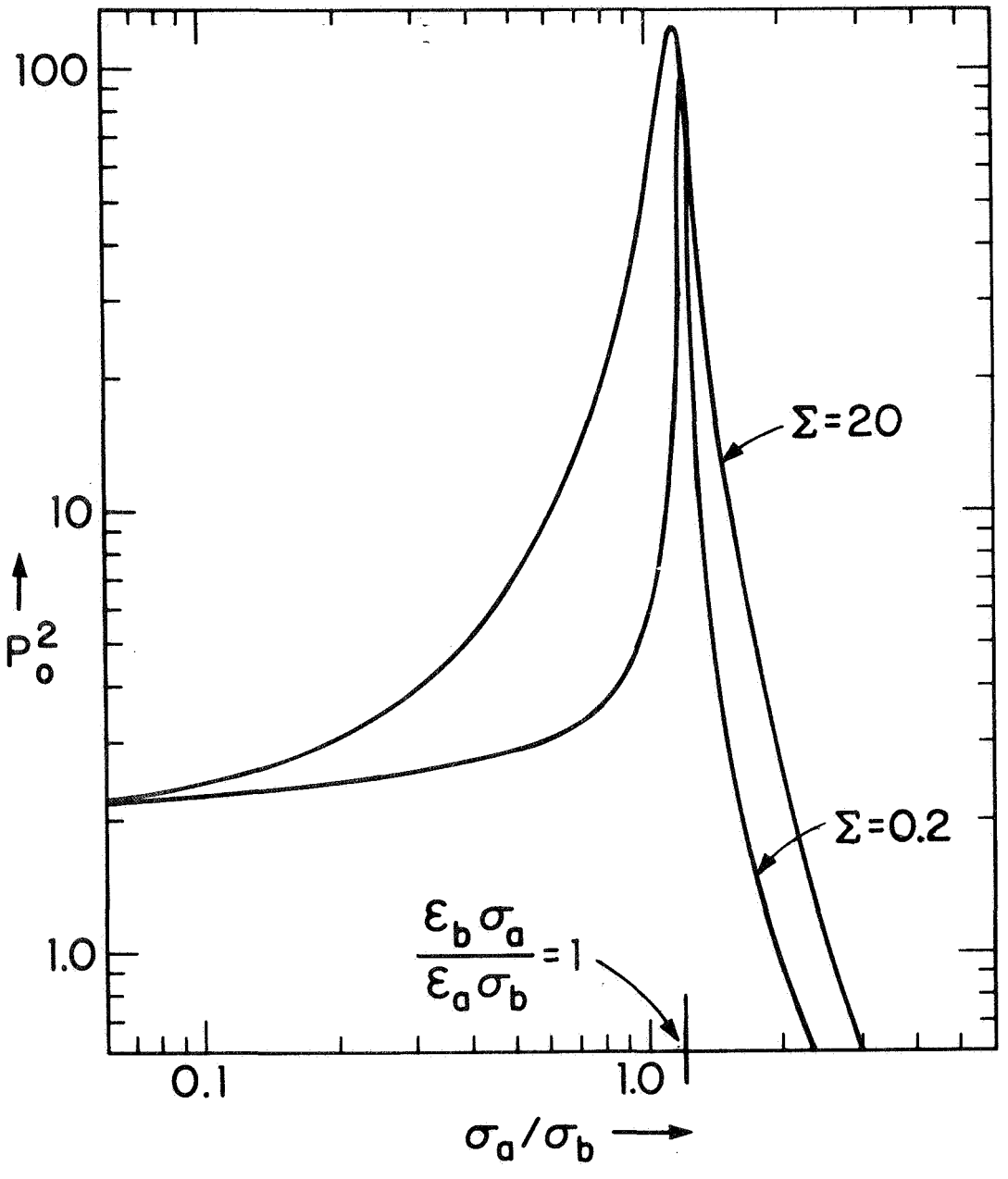

Fig. 6 Dependence of the normalized electric pressure P_o evaluated in the upper fluid on the ratio of conductivities. The parameter Σ is proportional to the sum of the viscosities and to the conductivity of the upper fluid. For these curves, $\varepsilon_a/\varepsilon_b = 1.22$.

static instability even in the absence of an equilibrium surface charge density. Note that this threshold is independent of the viscosity parameter Σ and, for small values of Σ, tends to be the peak value of P_o^2 as $\sigma_a/\sigma_b \to \epsilon_a/\epsilon_b$ (Fig. 6.).

VI. THEORETICAL OBSERVATIONS INCLUDING FINITE RELAXATION TIME EFFECTS

Even though the limiting situations of Secs. III - V differ greatly in terms of physical parameters, they have similarities in their dynamical behavior. In all cases, instabilities exhibit a purely exponential growth, and, for a wide range of physical parameters, the interface stressed by a dc field tends to behave as though it were infinitely conducting. Even with perfectly insulating liquids (Sec. IV), to a degree determined by the viscosity parameter $\underline{M}$, convection of equilibrium surface charge induced by interfacial shear stresses leads to instabilities with attributes approximating those for the perfectly conducting case of Sec. III.

In the opposite extreme of Sec. V, where relaxation is considered as instantaneous, it is found again that, unless the free charge density on the interface approaches zero, the incipience of instability is essentially as for the perfectly conducting interface. The degree to which this is true for a given ratio of conductivities depends on the viscosity parameter Σ; in the limit $\Sigma \to 0$, the range of conductivity ratios over which the perfectly conducting model fails to approximate the instability condition becomes vanishingly small.

As might be expected, a similar behavior is likely over a range of parameter values, even if the characteristic dynamical times $1/|s|$ are on the order of ϵ/σ for one or both of the fluids. This can be shown from a number of viewpoints, one of which is to take the limit of the dispersion equation (19) as the fluid viscosities become vanishingly small with the electric field finite. Then,

regardless of the liquid conductivities, Eq. (19) reduces to the dispersion equation for waves on a perfectly conducting interface between inviscid fluids.[2] Note that, if this limiting result is to be obtained by using an inviscid model at the outset, the boundary condition requiring conservation of charge at the interface must be ignored, and the condition of zero electric shear stress retained.

A quantitative statement of conditions under which the interface behaves as a perfectly conducting surface can be made in terms of an electric Hartmann number which generally depends on the particular combination of physical parameters, but takes the form[13]

$$H_e = \left[[\![\varepsilon E]\!]^2 / 8\mu(\sigma_a + \sigma_b) \right]^{1/2} \tag{40}$$

In Eq. (19), if the electric field intensity is sufficiently large that

$$\left| \frac{se}{kd} \right| << \left| \frac{\theta [\![\varepsilon E]\!]}{\rho_a + \rho_b} \right| \tag{41}$$

$$\left| \frac{2[\![\mu]\!]}{\rho_a + \rho_b} - \frac{sh}{kd} \right| << \left| \frac{\psi [\![\varepsilon E]\!]}{s(\rho_a + \rho_b)} \right| \tag{42}$$

and

$$\left| -\frac{sh}{kd} + \frac{2[\![\mu]\!]}{\rho_a + \rho_b} \right| << \left| \frac{\theta(\varepsilon_a E_a + \varepsilon_b E_b)}{(\rho_a + \rho_b)} \right| \tag{43}$$

then, regardless of the relaxation times, the dispersion equation reduces to

$$s^2 + gk(\alpha_b - \alpha_a) + \frac{Tk^3}{\rho_a + \rho_b} - \frac{k^2}{\rho_a + \rho_b} (\varepsilon_a E_a^2 + \varepsilon_b E_b^2) + \frac{eks^2}{d} = 0 \tag{44}$$

or that for a perfectly conducting, inviscid interface with an additional term to account for viscous damping. In this approximation, the electric shear

stresses dominate those due to viscosity. As a particular example, suppose that $\mu_a \approx \mu_b$ and $\rho_a \approx \rho_b$, so that $\nu_a \approx \nu_b$ and $q_a \approx q_b$. Then, conditions (42) and (43) are satisfied. If charge relaxation effects are to be important, then $s \gtrsim (\sigma_a + \sigma_b)/(\varepsilon_a + \varepsilon_b)$ and Eq. (41) is

$$\frac{s}{k(q-k)} << \frac{[\![\varepsilon E]\!]^2}{2\rho(\sigma_a + \sigma_b)} \tag{45}$$

To obtain a conservative estimate of whether or not the approximation is justified, $q - k \to s/2\nu k$ in Eq. (45). It follows that the interface responds essentially as a perfect conductor if H_e, as given by Eq. (40), is large compared to unity. In less particular instances, Eqs. (42) and (43) also require that electric Hartmann numbers be large.

VII. EXPERIMENTS

As indicated in the introduction, there are at least three experiments that give insight into the mechanisms of instability on the interfaces of highly insulating liquids. In all of these discussed here, the upper fluid is air or an electronegative gas, and the interfacial electric stress is established by means of a potential, V, applied between electrodes parallel to the interface and at $z = a$ and $z = -b$. Properties of the two liquids used are given in Table I: the relaxation times are in all cases in excess of 10 seconds. Effects of fringing fields are to a certain extent avoided by using the guard ring arrangement depicted in Fig. 7. The experiments differ in the temporal dependence of V.

A. Voltage Applied Gradually

First, consider the case where a dc voltage is established by raising the potential, V, at a rate low enough (over a period of a minute or more) to allow the equilibrium charge, Q, to relax to the interface. Then, the electric field intensity is excluded from the liquid so that $[\![E]\!] = E_a = V/a$ and, according to

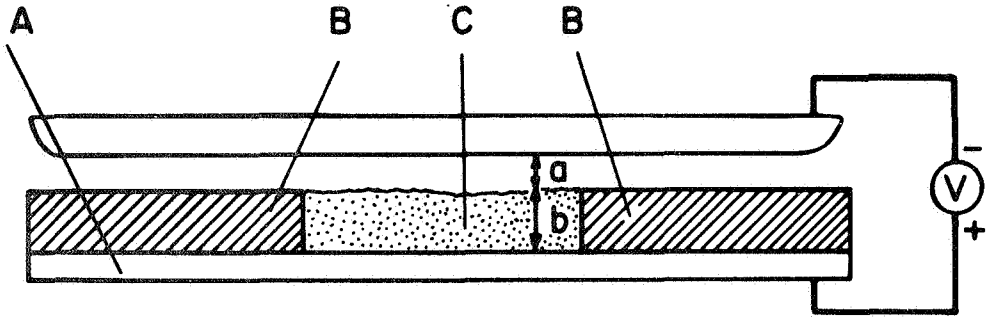

Fig. 7 Cross-sectional view of simple apparatus for measuring conditions for incipient instability. The liquid, C, is contained by a porous Balsa wood guard ring, B, saturated by liquid and as nearly as possible of the same electrical properties as the liquid, and a metal bottom electrode, A.

Eqs. (21) and (24), the interface becomes unstable as $V = V_s$, where

$$V_s = a[4\rho g T/\varepsilon_o^2]^{1/4} \tag{46}$$

It is convenient to picture this experiment in terms of the $\underline{P}$-$\underline{Q}$ plane of Fig. 3. By the definitions of $\underline{P}$ and $\underline{Q}$, Eqs. (28), this experiment is conducted along a path

$$\underline{P} = \sqrt{\kappa}\,\underline{Q} \tag{47}$$

in the $\underline{P}$-$\underline{Q}$ plane, with the equilibrium surface charge proportional to the applied voltage:

$$\underline{Q} = (V_o/a)[\varepsilon_o/Tk^*(1+\kappa)]^{1/2} \tag{48}$$

Thus, as the voltage is raised the experiment follows the trajectory A-B-D of Fig. 8. The instability condition, Eq. (46), is the voltage at which the trajectory intersects the ellipse.

The data point shown in Fig. 8 for this type of experiment is within 10% of the theoretically predicted value of $\underline{P}$. A more detailed comparison between theory and experiment is made possible by Figs. 9a and 9b, where the voltage for incipient instability is given as a function of the upper electrode-interface spacing, for both silicon oil (the liquid used for Fig. 8) and transformer oil. The curve denoted by "gradual" is predicted by Eq. (46).

B. Voltage Applied Suddenly

In the second experiment, a dc voltage is again raised slowly to follow the trajectory A-B of Fig. 8. Then, with $V = V_o$, where V_o is yet less than that given by Eq. (46), there is an equilibrium surface charge density on the interface given by Eq. (48) and the voltage is abruptly switched from V_o to V_p.

Fig. 8 Three experiments represented in the P-Q plane. With voltage raised gradually, trajectory A-B-D is followed, while if it is raised slowly and then increased abruptly, A-B-C is followed. With an ac voltage, the trajectory is A-F. Data and theoretical curves are for silicon oil.

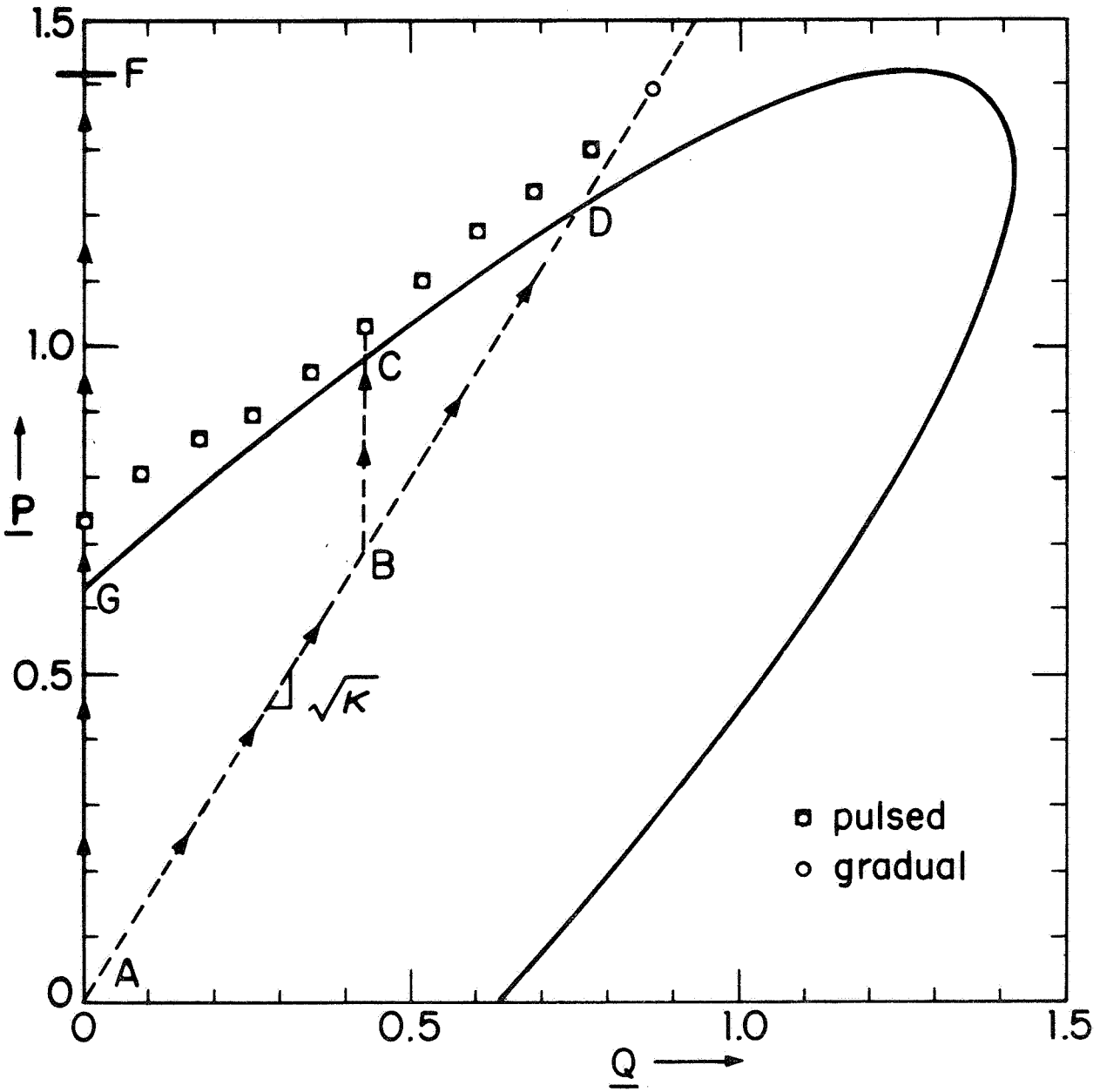

Thus, $\underline{Q}$ remains constant but $\underline{P}$ changes such that

$$[\![\varepsilon E]\!] = Q \quad ; \quad E_a a + E_b b = V_p \tag{49}$$

It follows that

$$\underline{P} = \sqrt{\varepsilon_o \kappa}\ [V_o(b/a + 1) + V_p(\kappa - 1)][k^* T(1+\kappa)(b + a\kappa)^2]^{-1/2} \tag{50}$$

and the experiment follows the trajectory B-C of Fig. 8. If V_p is increased so that trajectory B-C intersects the ellipse, instability is predicted by either Eq. (32) or (33).

The data denoted as "pulsed" in Fig. 8 are taken in this manner, again using silicon oil. Insofar as can be determined experimentally, the instability condition follows the elliptical contour of Fig. 8 within about 10%, even as $\underline{Q} \to 0$ (in the limit where the initial bias voltage $V_o = 0$). In fact, the data and curves of Figs. 9a and 9b denoted as "pulsed" are for this limiting case of $V_o = 0$, with the curves predicted by either Eq. (32) or (33), with $\underline{Q} = 0$!

C. Voltage Alternating at High Frequency

Now, consider the dielectrophoretic limit of no interfacial charge, Q, as obtained by applying a voltage of sufficiently high frequency (400 Hz) that charges do not have time to relax to the interface, and damping prevents a response of the liquid to the pulsating component of the electric stress. Then, according to Eq. (30), instability is incipient as $\underline{P} = \sqrt{2}$. This is shown as the pointF on the P axis in Fig. 8, a critical point that can be written in terms of the critical rms voltage $V = V_d$ by using Eq. (28) together with Eqs. (49), with $Q = 0$:

$$V_d = \frac{b + \kappa a}{\kappa - 1}\,[k^* 2T(\kappa + 1)/\varepsilon_o \kappa]^{1/2} \tag{51}$$

The predictions of this expression and data for two liquids are also shown in Figs. 9a and 9b, and are within experimental errors of each other.

Fig. 9 Three experiments of Fig. 8, showing dependence of instability voltage on the interface electrode spacing. In the pulsed case, the initial bias voltage is zero, corresponding to following the trajectory A-G of Fig. 8. The curves are predicted by the appropriate theoretical expressions. a) Silicon oil

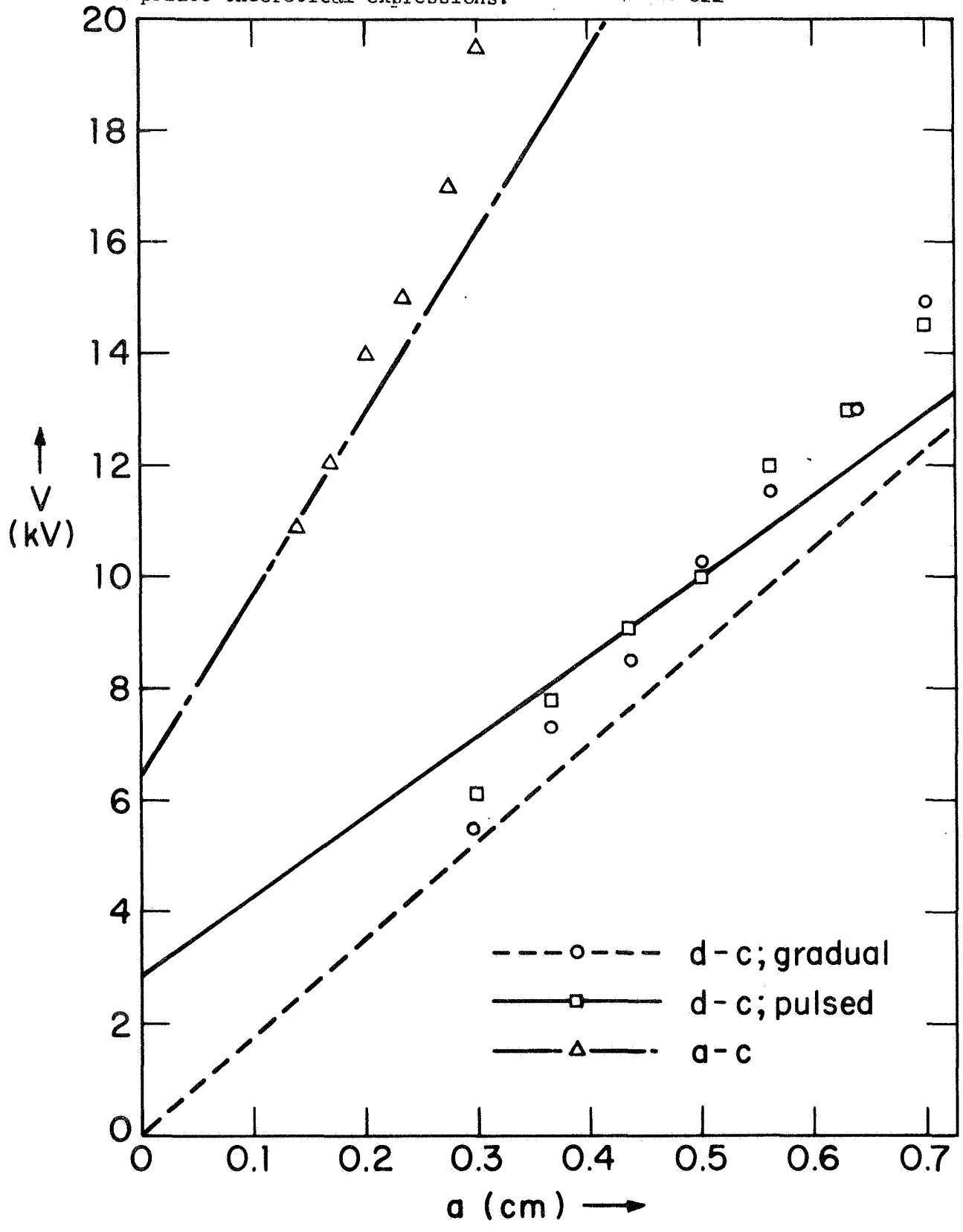

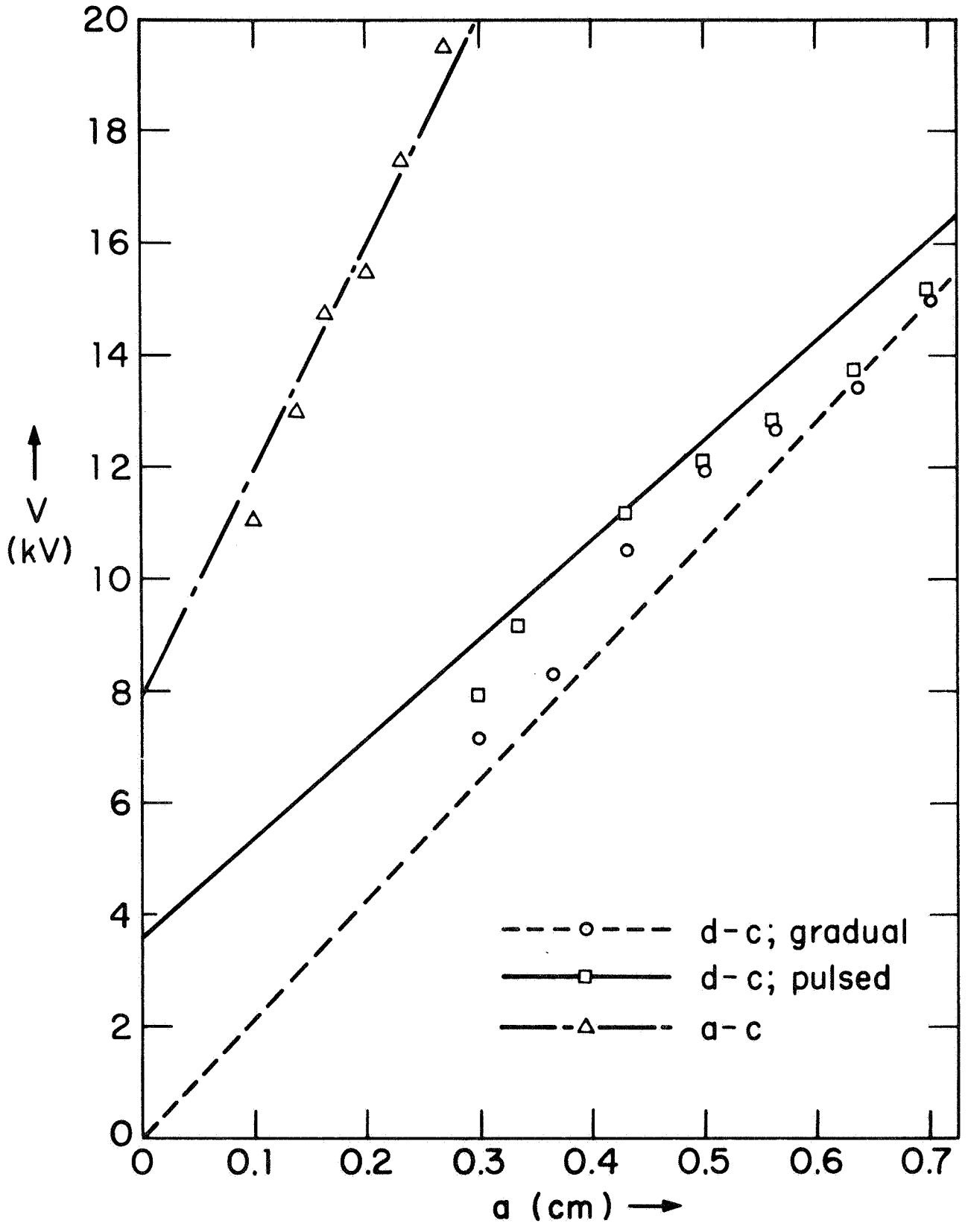

Fig. 9 b) Transformer oil

D. Discussion of Experiments

The difference between the theoretical thresholds for instability with the dc field voltage turned up slowly, and with it turned on abruptly, are not large. As Figs. 9a and 9b show, the experimental results for these two situations are essentially the same for all liquids tested, although there is a slight tendency for the pulsed experiments to require a higher voltage, as suggested by the theory.

By contrast, the critical voltage for the ac experiment is far higher than for either of the dc experiments, and within experimental errors of the appropriate theoretical curves. Thus, there is a clear verification that the dc transient experiment does not approach the dielectrophoretic limit as the initial bias voltage (and hence, presumably, the initial interfacial surface charge) approaches zero.

It is essential to recognize that the electrical relaxation times of both liquids (Table I) are much longer than the time required for observation of instability in the pulsed experiment. These relaxation times can be established in several ways, including conductivity cell measurements and electromechanical resonance techniques.[14] However, the most direct of these is simply to replace the upper electrode (Fig. 7) with a flexible cantilevered foil strip which acts as an electrometer movement. With the voltage applied suddenly, the metal strip abruptly moves downward in response to the charging current, but then continues to move downward with a time constant of 10 or more seconds, asymptotically approaching a static equilibrium. A recording of this latter motion reflects the time required for establishing that part of the force due to images of the equilibrium free charge on the interface.

The difference between the results with the abrupt application of a constant voltage and with an ac voltage is attributable to the extreme sensitivity

of the instability condition to small amounts of equilibrium surface charge. This is illustrated by Fig. 5, where the contour of constant growth rate for $\underline{M} = 3.34 \times 10^{-2}$ is for the case of transformer oil. In terms of actual time, the growth rate $\underline{s} = 0.2$ corresponds to an instability time constant of 7.5×10^{-2} sec. Through the mechanism of the interfacial shear stress, even a small amount of interfacial equilibrium charge is extremely influential in determining incipience of instability with these liquids. For a time constant of 0.1 seconds, the contour of constant growth rate is very nearly the ellipse, except in the immediate vicinity of the $\underline{P}$ axis. In spite of the extremely long time constant for establishing the equilibrium surface charge, only a small portion of that charge is required to make the interface behave like a perfectly conducting deformable surface. Even more, this small fraction of the charge can probably be characterized by a shorter time constant than for the majority of carriers. It is likely that several mechanisms for electrical conduction, each with its own characteristic time constant, are at work in the commercial grade liquids used, and it is the longest time constant that is referred to here. Moreover, it is possible that the interfaces support a residual free charge.

VIII CONCLUDING REMARKS

In the last four sections, several viewpoints are used to emphasize, theoretically and experimentally, the important consequences of the electrical shear surface force densities induced in various situations on a deforming interface stressed by an initially perpendicular electric field - forces that bring into play viscous shear stresses and the convection of surface charge. For liquids of low or moderate viscosity, these shear forces tend to induce that convection of the interfacial free charge required to make the electrical interfacial shear stresses vanish. Thus, the interface tends to behave as a perfectly

conducting surface, with the charge convection replacing the conduction and the electric field tending to induce static (aperiodic) instability.

This work complements investigations previously reported in which the equilibrium field is tangential to the interface.[7] In that work it was shown that a large electric Hartmann number generally implies overstability. By contrast, in the case presented here, static instability is implied by a large electric Hartmann number regardless of the electrical relaxation time.

Finally, it should not be overlooked that useful results on the effects of viscosity on growth rates of instability, with and without the influence of charge relaxation, are a byproduct of the development.

Acknowledgment:

The authors are indebted to Mr. Tsen-Chung Chen for obtaining most of the experimental data. This work was supported by NASA Grant NGL-22-009-014#6.

TABLE I Liquid Properties

Properties Used in MKS Units	Dow Corning 200 Series Silicon Oil	G.E. 10C Transformer Oil
Relative permittivity, κ	2.63	2.56
Surface tension, T	2.01×10^{-2}	$\approx 4 \times 10^{-2}$
Viscosity, μ	$\approx 10^{-2}$	$\approx 10^{-2}$
Density, ρ	0.94×10^{3}	0.87×10^{3}
Relaxation time, ϵ/σ	> 10 secs.	> 40 secs.

References

1. G. I. Taylor and A. D. McEwan, J. Fluid Mech., 22, 1 (1965).

2. J. R. Melcher, Field-Coupled Surface Waves (M.I.T. Press, Cambridge, Mass., 1963) Chaps. 3 and 4.

3. J. R. Melcher and E. P. Warren, Phys. Fluids, 9, 2085 (1966).

4. See Ref. 2, p. 39

5. E. B. Devitt and J. R. Melcher, Phys. Fluids, 8, 1193 (1965).

6. For a discussion of cases where bulk forces do arise in ohmic fluids, see J. R. Melcher and M.S. Firebaugh, Phys. Fluids, 10, 1178 (1967).

7. J. R. Melcher and W. J. Schwarz, Jr., To be published, Phys. Fluids.

8. R. J. Raco, "Stability of a Fluid Interface in the Presence of a Transverse Electrostatic Field", (Ph.D. Thesis, Rutgers University, New Brunswick, N. J., 1966).

9. J. M. Reynolds, Phys. Fluids, 8, 161 (1965).

10. P. J. Cressman, J. Appl. Phys., 34, 2327 (1963).

11. H. F. Budd, J. Appl. Phys., 36, 1613 (1965).

12. S. Chandrasekhar, Hydrodynamic and Hydromagnetic Stability (Oxford Press, London, 1961) p. 94.

13. J. R. Melcher and G. I. Taylor, "Electrohydrodynamics: A Review of the Role of Interfacial Shear Stresses", Chapter in Annual Review of Fluid Mechanics, Vol. I (1969) in publication.

14. J. R. Melcher, Phys. Fluids, 10, 325 (1967).

Fig. 1 Configuration of interface and applied electric field intensity.

Fig. 2a Complex normalized frequency, $\underline{s}$, as a function of normalized wave-number, $\underline{k}$, for cases of zero electrical shear stress. Onset of instability occurs as the normalized electric pressure $\underline{P} = \sqrt{2}$ so that a stable and an unstable case are shown. The normalized viscosity $\underline{M} = 3.34 \times 10^{-2}$, illustrative of transformer oil with $\rho = 0.87 \times 10^{3} kg/m^{3}$, $T = 4 \times 10^{-2} n./m.$, $\mu = 9.15 \times 10^{-3} N\text{-}sec/m^{2}$.

Fig. 2b Parameters as in (a), except that $\underline{M} = 3.34$, to illustrate high viscosity effect.

Fig. 3 Regime of stability in the $\underline{P}$-$\underline{Q}$ plane, where $\underline{Q}$ is the normalized surface charge and $\underline{P}$ is the normalized jump in electric field intensity at the interface. As $\underline{P}$ is raised with $\underline{Q} = 0$, polarization (dielectrophoretic) instability occurs at A, while the free charge instability occurs (asymptotically) at B. Raising the voltage slowly gives the trajectory shown, with instability at the point C. $\kappa = 2.56$, characteristic of transformer oil.

Fig. 4 Normalized complex frequencies, $\underline{s}$, as a function of surface charge density, $\underline{Q}$. Points (a) - (c) correspond to those shown on Fig. 3, where $\underline{P} = 1$.

a) The viscosity is that of transformer oil, $\underline{M} = 3.34 \times 10^{-2}$. From (a)-(b) and beyond (c), there are a complex conjugate pair of roots and a purely positive real root. From (b)-(c) there are two complex conjugate pairs of roots.

b) Viscosity parameter $\underline{M} = 3.34$. From (a)-(b) and beyond (c), there are three purely real roots, one corresponding to instability. From (b)-(c) there are three roots representing damping. The third root, now shown, is essentially constant at $\underline{s} = 3$.

Fig. 5 Contours of constant growth rate $\underline{s}$ = 0.2, $\underline{k}$ = 1.0 in the $\underline{P}$-$\underline{Q}$ plane as a function of the viscosity parameter, $\underline{M}$. In the limit of zero viscosity, the contour becomes the marginal stability curve of Fig. 3; κ = 2.56.

Fig. 6 Dependence of the normalized electric pressure P_o evaluated in the upper fluid on the ratio of conductivities. The parameter Σ is proportional to the sum of the viscosities and to the conductivity of the upper fluid. For these curves, $\varepsilon_a/\varepsilon_b$ = 1.22.

Fig. 7 Cross-sectional view of simple apparatus for measuring conditions for incipient instability. The liquid, C, is contained by a porous Balsa wood guard ring, B, saturated by liquid and as nearly as possible of the same electrical properties as the liquid, and a metal bottom electrode, A.

Fig. 8 Three experiments represented in the $\underline{P}$-$\underline{Q}$ plane. With voltage raised gradually, trajectory A-B-D is followed, while if it is raised slowly and then increased abruptly, A-B-C is followed. With an ac voltage, the trajectory is A-F. Data and theoretical curves are for silicon oil.

Fig. 9 Three experiments of Fig. 8, showing dependence of instability voltage on the interface electrode spacing. In the pulsed case, the initial bias voltage is zero, corresponding to following the trajectory A-G of Fig. 8. The curves are predicted by the appropriate theoretical expressions.

a) Silicon oil

b) Transformer oil